

Dependence of Surface Strain on Geometry in Embedded Quantum-Dot Systems

Jianxin Zhong¹, Jack C. Wells¹, Qian Niu², and Zhenyu Zhang³

¹*Center for Engineering Science Advanced Research and Computer Science and Mathematics Division, Oak Ridge National Laboratory, Oak Ridge, TN 37831-6355*

²*Department of Physics, University of Texas at Austin, Austin, Texas 78712*

³*Solid State Division, Oak Ridge National Laboratory, Oak Ridge, TN 37831*

(Dated: February 18, 2002)

Strain fields induced by embedded islands of pyramidal shape are examined by analyzing Ge/Si systems using the continuum theory of elasticity. We show that, upon increasing spacer thickness, the decay of the strain field on the spacer surface undergoes a crossover from a non-cubic inverse power law to a cubic inverse power law. The exponent for the non-cubic inverse power law depends on island slope with a smaller slope corresponding to a smaller exponent. Additionally, the strain is nearly proportional to the island volume when the slope is large but to the island area when the slope is small. This work provides a consistent theoretical context for understanding the diverse strain properties of these systems previously obtained by large-scale atomistic simulations.

PACS numbers: Valid PACS appear here

Quantum dot arrays have many important technological applications. Strain-driven formation of nanoscale coherent islands on lattice-mismatched layers in heteroepitaxy offers an attractive way for effective fabrication of quantum dots of large density [1, 2]. Normally, these islands are not well organized in space and show large dispersion in size distribution. Recent experiments showed that the spatial ordering and size uniformity of islands can be greatly improved by growing multilayers of islands separated with spacer layers [3–9]. Vertical alignment of islands was found in semiconductor systems including InAs/GaAs [3, 4] and Ge/Si [5], and also in magnetic systems including Co/Au [6]. Taking advantage of the anisotropic nature of strain fields in some semiconductor materials, anticorrelation of island positions and a fcc-like structure of islands was observed in CdZnSe/ZnSe [7] and in PbSe/PbEuTe [8], respectively.

The self-organization of the stacked islands is believed to be a result of the strain field on spacer surfaces induced by embedded islands. This was demonstrated by analyzing the net atomic current to the locations of strain concentration due to strain-biased diffusion [3], by analyzing the strain modulation of nucleation centers [9], and by kinetic Monte-Carlo simulations [10, 11]. In these studies [3, 9–11], an embedded island is modeled as a force dipole of zero dimension within the continuum theory of elasticity that gives strain and stress fields characterized by a cubic inverse power-law dependence on spacer thickness and a linear dependence on island volume. The force dipole model is questionable because islands have spatial occupations of finite dimensions and show no cubic or spherical symmetry. The influence of island dimension on surface strain must be considered in order to achieve quantitative description of the growth process [12, 13].

Three different approaches have been used in calculating strain fields for embedded islands of finite dimensions. The first one is the Green function method within continuum theory [14, 15], using the solution for a force dipole as the Green function. The second approach involves

continuum finite element calculations, which was shown to give the same results as Green function method [15]. An attractive advantage of the Green function method is that the strain induced by a large number of embedded islands can be simply calculated by superposition of the contribution from each island. However, it is an open question whether the Green function method is still reliable for systems of nanoscale spacer thickness. The third approach [16, 17] emphasizes the discrete atomic nature and utilizes atomistic simulation methods such as molecular dynamics simulations, which can provide accurate results but is very computationally demanding. Two completely different results from such large scale atomistic simulations were reported recently [16, 17] for the stress fields at Si spacer surfaces induced by Ge islands of the pyramidal shape suggested by experiments [18]. One claimed that [16] the stress field can be well approximated by the force dipole model. The other found that [17] the stress field deviates significantly from the description of the force dipole, exhibiting a nearly linear inverse dependence on spacer thickness and a linear dependence on island surface area.

In this letter, we provide a clear understanding of these “apparently inconsistent” predictions from atomistic simulations. Specifically, we examine the dependence of surface strain on island geometry by analyzing pyramidal Ge islands embedded in Si using the Green function method. We show that, upon increasing spacer thickness, the decay of the strain field on the spacer surface exhibits a crossover behavior from a non-cubic inverse power law to a cubic inverse power law. The exponents for the non-cubic inverse power laws depend on island slopes with smaller slopes corresponding to smaller exponents. The strain dependence on island size also displays interesting behaviors when the spacer thickness is small, compared with island base-width. The strain field has a nearly linear dependence on island volume when the island slope is large but has a nearly linear dependence on island surface area if the island slope is small. Our findings are

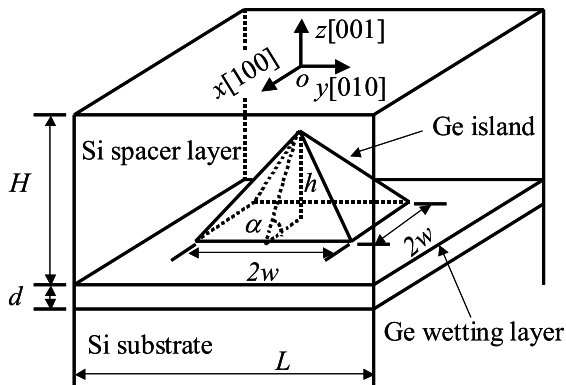


FIG. 1: Schematic illustration of the system. A germanium island of pyramidal shape with a germanium wetting layer above a silicon substrate is capped by a spacer layer of silicon.

consistent with the results from atomistic simulations, demonstrating the utility of the continuum theory for embedded quantum-dot systems. Based on our results, the “discrepancy” derived from the atomistic simulations, namely, whether the strain distribution of a pyramidal Ge island in Si can or cannot be modeled by a force dipole, can be well understood by noticing the geometry difference of the islands in those simulations. We believe that the broad theoretical framework and the clear elucidation of the nature of the surface strain presented in this work have significant importance in future studies of the growth process and physical properties of these systems.

The unit cell of our system is schematically shown in Fig. 1. A pyramidal Ge island with an initially formed wetting layer of thickness d on a Si(001) substrate is capped by a Si spacer layer of thickness H . The base of the pyramid is a square of width $2w$, oriented in [100] and [010] directions. Island height is given by $h = w \times \tan \alpha$, where α is the slope angle. The wetting layer is always very thin (about 3 monolayers for Ge/Si) and its contribution to the strain field at the spacer surface is only a small constant. We neglect it by choosing $d = 0$. The periodicity of the system is L , and $L \rightarrow \infty$ gives a system which consists of only one embedded island.

We start our analysis for a single Ge island of volume V embedded in Si. In continuum theory, an embedded island can be modeled as an inclusion and can be further treated as a collection of individual force dipoles of infinitesimal size dV comprising the volume V . The strain field outside of the island is then given by the superposition of the contribution from each force dipole. In other words, the strain field for a force dipole is the Green function for the strain field of the island. Suppose a force dipole with $dV = dx'dy'dz'$ is located at position (x', y', z') in an isotropic material such as Si, one can show that [19] the trace of the strain tensor,

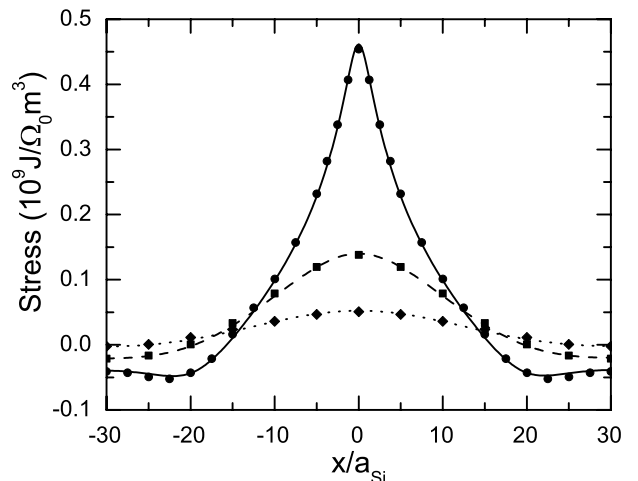


FIG. 2: Stress σ at $y = z = 0$ as a function of x for embedded islands with $w = 20a_{\text{Si}}$, $h = 17\text{ML}$, and $L = 60a_{\text{Si}}$. Symbols are results from the reference [17] obtained by atomistic simulations. Circles, squares, and diamonds correspond to spacer thickness $H = 21\text{ML}$, 49ML , and 81ML , respectively. Lines are results of calculations using Green function method.

$G = G_{xx} + G_{yy} + G_{zz}$, at the spacer surface is given by

$$G = -\frac{\epsilon_0(1+\nu)(1-2\nu)dV}{\pi(1-\nu)}\left(1 - \frac{3z'^2}{R^2}\right)/R^3, \quad (1)$$

where $R = \sqrt{(x-x')^2 + (y-y')^2 + z'^2}$, ν is Poisson's ratio of the spacer material, and ϵ_0 the lattice misfit with $\epsilon_0 = (a_i - a_s)/a_i$. Here, a_i and a_s are the lattice constants for the inclusion and spacer materials, respectively. The strain field ϵ for the embedded island is then given by the integration of the Green function in Eq. (1) over the volume of the island [14, 15, 19], namely, $\epsilon = \int_V G(x', y', z') dx' dy' dz'$. The trace of the stress tensor reads $\sigma = \frac{E}{1-2\nu}\epsilon$, where E is the Young's modulus. The strain and stress fields for arrays of embedded islands can be obtained further by superposition of the contribution from each island. In our calculations for Ge/Si systems, we have $a_i = a_{\text{Ge}} = 5.656\text{\AA}$ and $a_s = a_{\text{Si}} = 5.431\text{\AA}$. We choose $\nu = 0.218$ as used in the reference [16].

In Fig. 2, we compare our calculations for the stress fields for a periodic lattice of embedded Ge islands with $L = 60a_{\text{Si}}$ to the results from atomistic simulations. The Ge islands have pyramidal shape of $\{105\}$ facets with $w = 20a_{\text{Si}}$ and $h = 17\text{ML}$. Symbols in Fig. 2 are from the atomistic simulations [17] after removal of the contribution coming from the spacer surface reconstruction by subtraction of a constant term p_d [17]. Lines are our results using $E = 8.404 \times 10^9 \text{J}/\Omega_0 m^3$, $10.152 \times 10^9 \text{J}/\Omega_0 m^3$, and $10.152 \times 10^9 \text{J}/\Omega_0 m^3$ for $H = 21\text{ML}$, 49ML , and 81ML , respectively, which gives an excellent fit to the results of atomistic simulations. Here, $\Omega_0 = \Omega/a_{\text{Si}}^3$ is the dimensionless average atomic volume [17]. The constant term p_d is the stress associated with the surface dimerization. The fit shown in Fig. 2 leads to $p_d =$

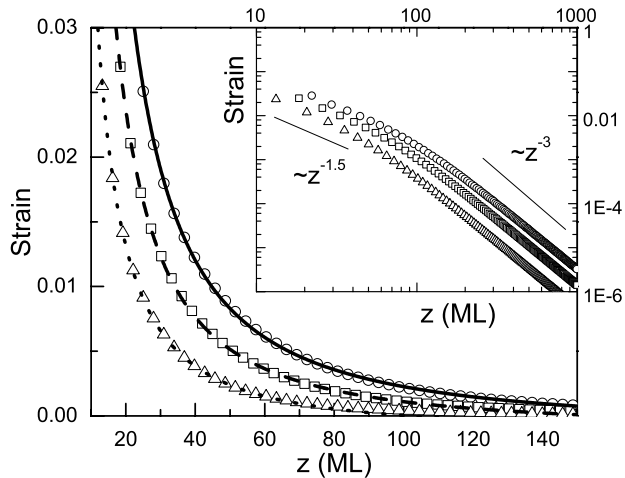


FIG. 3: Strain ϵ at $x = y = 0$ as a function of spacer thickness. Circles, squares, and triangles correspond to islands with $(w, h) = (20a_{\text{Si}}, 17\text{ML})$, $(15a_{\text{Si}}, 13\text{ML})$, and $(10a_{\text{Si}}, 9\text{ML})$, respectively. Thick lines are corresponding fitting results that give $\epsilon = a_0 + a_1/z^{1.50}$ with $(a_0, a_1) = (-1.26 \times 10^{-3}, 1.29)$, $(-9.20 \times 10^{-4}, 2.06)$, and $(-1.04 \times 10^{-3}, 3.30)$. Inset shows the crossover behavior upon increasing the spacer thickness from small separation regime to large separation regime.

$0.754(10^9\text{J}/\Omega_0 m^3)$, which is very close to the approximate value $0.747(10^9\text{J}/\Omega_0 m^3)$ obtained in atomistic simulations [17]. We notice that the Young's modulus takes a different value when the Si spacer layer is thin such as 21ML. This may be attributed to the slight change of the mechanical properties of the Si material when the spacer surface is so close to the island. We also performed calculations for a single embedded Ge island ($L \rightarrow \infty$) and found that the local surface stress fields at the location directly above the island in these two systems with $L = 60a_{\text{Si}}$ and $L \rightarrow \infty$ differ by a small amount, indicating that the strain and stress fields decay sufficiently fast that the nearest-neighbor sites are negligible. In the following, we focus on analyzing the surface strain induced by single embedded Ge islands.

Fig. 3 illustrates the strain at $x = y = 0$ as a function of spacer thickness. Symbols are our results from Green function method for single pyramidal Ge islands with $\{10\bar{5}\}$ facets of three different sizes. Inset of Fig. 3 is the log-log plot of the strain versus spacer thickness from the small separation regime to the large separation regime. Circles, squares, and triangles correspond to islands described by $(w, h) = (20a_{\text{Si}}, 17\text{ML})$, $(15a_{\text{Si}}, 13\text{ML})$, and $(10a_{\text{Si}}, 9\text{ML})$, respectively. Thick lines are the fitting results in the small separation regime that give $\epsilon = a_0 + a_1/z^\gamma$ with $\gamma = 1.50$ and corresponding parameters $(a_0, a_1) = (-1.26 \times 10^{-3}, 1.29)$, $(-9.20 \times 10^{-4}, 2.06)$, and $(-1.04 \times 10^{-3}, 3.30)$. Another exponent $\gamma \approx 1$ was found for the same islands in atomistic simulations [17], where less data points were used for fitting. Our results based on large number of data points show that the best fit gives $\gamma = 1.50$. Moreover, the Green function method

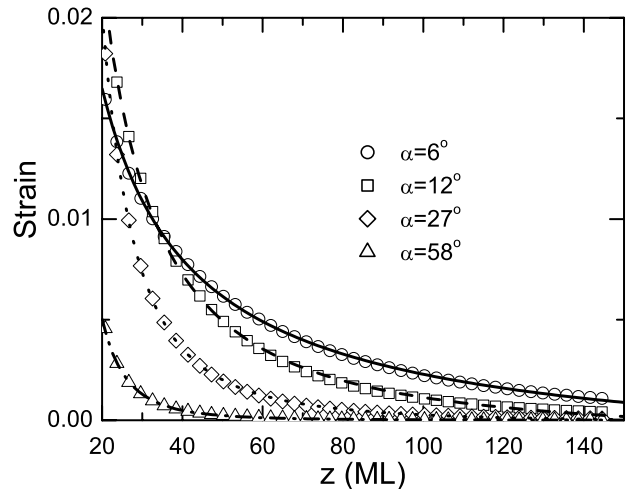


FIG. 4: Strain ϵ at $x = y = 0$ as a function of spacer layer thickness. Circles, squares, diamonds, and triangles correspond to systems with slope angles $\alpha = 6^\circ$, 12° , 27° , and 58° , respectively. Lines show fitting results that give $\epsilon = a_0 + a_1/z^\gamma$ with $(a_0, a_1, \alpha) = (-2.48 \times 10^{-3}, 0.25, 0.86)$, $(-9.20 \times 10^{-4}, 2.06, 1.50)$, $(-1.10 \times 10^{-4}, 33.02, 2.47)$, and $(2.78 \times 10^{-6}, 116.78, 3.36)$, respectively.

allows us to deal with the large separation regime where the application of atomistic simulations is not possible so far. The inset of Fig. 3 shows that, upon increasing the spacer thickness, the decay of the strain field exhibits a crossover behavior from $\gamma = 1.5$ to $\gamma = 3$.

We find that the exponent γ is a function of island slope with a larger slope corresponding to a larger exponent. We show in Fig. 4 the decay behavior of the strain fields for four pyramidal islands of different slopes, where circles, squares, diamonds, and triangles are results for islands with $(w, h) = (30a_{\text{Si}}, 13\text{ML})$, $(15a_{\text{Si}}, 13\text{ML})$, $(6.5a_{\text{Si}}, 13\text{ML})$, and $(2a_{\text{Si}}, 13\text{ML})$, respectively, corresponding to slope angles $\alpha = 6^\circ$, 12° , 27° , and 58° . The decay can be well fitted to $\epsilon = a_0 + a_1/z^\gamma$ with $(a_0, a_1, \alpha) = (-2.48 \times 10^{-3}, 0.25, 0.86)$, $(-9.20 \times 10^{-4}, 2.06, 1.50)$, $(-1.10 \times 10^{-4}, 33.02, 2.47)$, and $(2.78 \times 10^{-6}, 116.78, 3.36)$, respectively. Atomistic simulations found that [16] the strain for a pyramidal island with $w = 5.6\text{nm}$ and $h = 2.8\text{nm}$ ($\alpha = 27^\circ$) can be approximated by the force dipole model with $\gamma = 3$. Our calculations give $\gamma = 2.47$ close to $\gamma = 3$.

The strain dependence on island size also displays interesting behaviors for islands of different slopes. Fig. 5 illustrates the strain fields at position $x = y = z = 0$ as a function of island width for pyramidal islands of different slopes embedded at $H = 81\text{ML}$. The strain is normalized by the island surface area $s = 4w \times h / \sin(\alpha)$. It is clear that when the island width is small compared to the spacer thickness, the normalized strain is always proportional to the island width, showing a linear dependence of the strain on island volume consistent with the force dipole model. However, for islands of large sizes

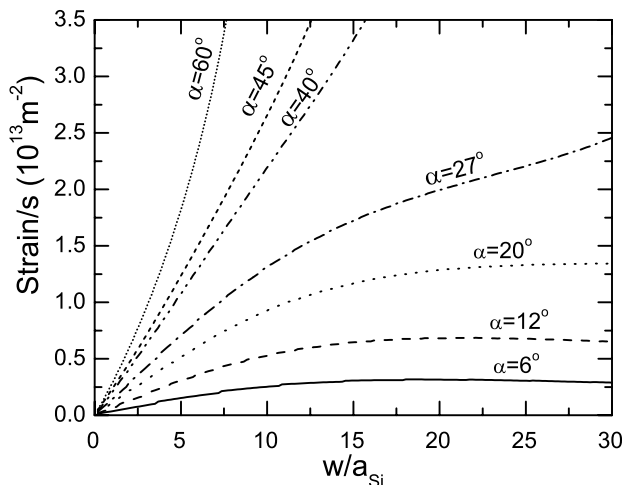


FIG. 5: Normalized strain ϵ/s at $x = y = z = 0$ as a function of island width for islands of different slopes with $H = 81\text{ML}$.

compared with the spacer thickness, the strain dependence on island size critically depends on island slope. For islands with small slope angles $\alpha < 20^\circ$, the normalized strain changes very slowly with the island width, indicating that the strain is nearly proportional to the island surface area. Differently, for $20^\circ < \alpha < 45^\circ$, the normalized strain is proportional to the width, giving a volume dependence similar to the case for small islands. For islands with $\alpha > 45^\circ$, a super linear dependence of strain on island volume exists. In a recent publication [17], molecular dynamics simulation was used to analyze the strain fields induced by pyramidal Ge islands of three different sizes $(w, h) = (20a_{\text{Si}}, 17\text{ML})$, $(15a_{\text{Si}}, 13\text{ML})$, and $(10a_{\text{Si}}, 9\text{ML})$, all have a slope angle $\alpha = 12^\circ$. For these islands, Fig. 5 predicts that the strain is nearly propor-

tional to the island surface area, consistent with the observation in atomistic simulations [17]. In another publication [16], a Ge island of $\alpha = 27^\circ$ with size $w = 5.6\text{nm}$ and $h = 2.8\text{nm}$ was investigated. In this case, the prediction from Fig. 5 of a nearly linear strain dependence on island volume is again in consistent with the atomistic simulations.

In summary, we have examined the strain fields on spacer layer surfaces induced by embedded islands of pyramidal shape by analyzing Ge/Si systems in the framework of continuum theory. We found that the diverse properties of the strain fields for these systems obtained previously by atomistic simulations can be well described by the continuum theory after integrating the influence of the island geometry using the Green function method. Our results clearly show that in the regime of small spacer thickness, the strain fields depend critically on island geometry, with smaller island slopes corresponding to larger deviations from the description of the force dipole model. We emphasize that, in the large separation regime, the force dipole approximation is consistent with our results, as one would expect when the island size is negligible compared to the spacer thickness. However, it is the small separation regime that is interesting and important for applications, and it is within this regime that the effects of finite dimensions and island geometry must be considered.

Acknowledgments

This work was supported by the Material Sciences and Engineering Division Program of the DOE Office of Science under contract DE-AC05-00OR22725 with UT-Battelle, LLC, and by the US National Science Foundation under Grants No. DMR-0071893.

-
- [1] D. Leonard *et al.*, Appl. Phys. Lett. **63**, 3203 (1993).
 - [2] J.M. Moison *et al.*, Appl. Phys. Lett. **64**, 196 (1994).
 - [3] Q. Xie, A. Madhukar, P. Chen, and N. Kobayashi, Phys. Rev. Lett. **75**, 2542 (1995).
 - [4] G.S. Solomon, J.A. Trezza, A.F. Marshall, and J.S. Harris, Phys. Rev. Lett. **76**, 952 (1996).
 - [5] C. Teichert, L.J. Peticolas, J.C. Bean, J. Tersoff, and M.G. Lagally, Phys. Rev. B **53**, 16334 (1996); P. Schittenhelm *et al.*, J. Vac. Sci. Technol. B **16**, 1575 (1998).
 - [6] O. Fruchart, M. Klaua, J. Barthel, and J. Kirschner, Phys. Rev. Lett. **83**, 2769 (1999).
 - [7] M. Strassburg *et al.*, Appl. Phys. Lett. **72**, 942 (1998).
 - [8] G. Springholz, V. Holy, M. Pinczolits, and G. Bauer, Science **282**, 734 (1998); V. Holy, G. Springholz, M. Pinczolits, and G. Bauer, Phys. Rev. Lett. **83**, 356 (1999).
 - [9] J. Tersoff, C. Teichert, and M.G. Lagally, Phys. Rev. Lett. **76**, 1675 (1996).
 - [10] C.-S. Lee, B. Kahang, and A.-L. Barabási, Appl. Phys. Lett. **78**, 984 (2001).
 - [11] P.M. Lam and S. Tan, Phys. Rev. B **64**, 035321 (2001).
 - [12] F. Liu, S.E. Davenport, H. M. Evans, and M.G. Lagally, Phys. Rev. Lett. **82**, 2528 (1999).
 - [13] G. Springholz *et al.* Phy. Rev. Lett. **84**, 4669 (2000).
 - [14] J.R. Downes, D.A. Faux, and E.P. O'Reilly, J. Appl. Phys. **81**, 6700 (1997).
 - [15] A.E. Romanov, G.E. Beltz, W.T. Fischer, P.M. Petroff, and J.S. Speck, J. Appl. Phys. **89**, 4523 (2001).
 - [16] I. Daruka *et al.*, Phys. Rev. B **60**, R2150 (1999).
 - [17] M.A. Makeev and A. Madhukar, Phys. Rev. Lett. **86**, 5542 (2001).
 - [18] J.L. Bischoff *et al.*, Mat. Sci. Eng. B **69-70**, 374 (2000); P. Sutter and M.G. Lagally, Phys. Rev. Lett. **81**, 3471 (1998); M. Grundmann, O. Stier, and D. Bimberg, Phys. Rev. B **52**, 11 969 (1995);
 - [19] R.D. Mindlin and D.H. Cheng, J. Appl. Phys. **21**, 926 (1950); A.A. Maradudin and R.F. Wallis, Surf.Sci. **91**, 423 (1980); S.M. Hu, J. Appl. Phys. **66**, 2741 (1989).